Chapter - 4

Analysis Methods

4.1. Introduction

The data recorded have been analysed by constructing a series of one- and two-dimensional spectra, correlating data from different parts of the detector setup. New generation of higher efficiency γ-detector arrays have made possible the collection of higher fold coincidence data in appreciable quantities in a relatively short time. The unsurpassed sensitivity and resolving power of such arrays has rejuvenated the field of nuclear structure physics at the extremes of angular momentum and isospin. The data size and the contents from such systems have increased to greater extents, making it imperative to automatize not only the data sorting and analysis, but also the pre-sorting of data. The primary aim of the in-beam γ-ray experiment is to deduce the level scheme of a nucleus using the γ^N coincidence data set, where N is the dimension of the data set, which is usually governed by the coincidence-fold set during the data acquisition. A systematic procedure has been adopted for detailed off-line analysis of the acquired data. During the pre-sorting of the acquired data, instrumental drifts, if any, were corrected for. The add-back spectra were obtained after appropriate gain matching. Higher fold data was un-folded into the corresponding two-fold events. From this data the conventional E_γ-E_γ histograms (symmetric as well as angle-dependent) were generated. In this chapter, the techniques in the data analysis are described, along with the conditions and selections applied to the data in order to create histograms. The main objectives of data analysis in γ-ray spectroscopy are:

- Look for γ-transitions following the nuclear reaction.
- Look for correlations γ-γ, γ-γ-γ etc, to search for sequence of transitions.
- Measure the intensity of each transition to estimate the population of each level.
- Extract angular distribution, angular correlation and polarization of the γ-transitions.
- Establish the level scheme, spin and parity of each level.
- Additional information like life times of the states can be extracted which gives valuable information about nuclear matrix elements.

4.2. Pre-sorting of the Raw Data

Data from multi-Clover arrays are generally sorted in 'list mode' format where all the parameters associated with an event (i.e. energy and timing from each detector) along with some identification tags are recorded event by event. To minimize storage space, the data may be condensed by eliminating zero channels. To reduced overheads, one record may contain data from several successful events.

During analysis, the data records are read back and unpacked to retrieve the original ADC values associated with each event. At this stage data are checked for inconsistency like malfunctioning of detectors and bad data sectors. Starting from an energy calibration provided by radioactive sources, calibrated singles spectra for each detector are generated. Strong lines in the coincidence data sets can be used for internal calibration and to correct for any gradual drift in amplifier gain. In a multi-Clover array, detectors placed at different angles are essentially equivalent. Data from different detectors can therefore be combined together to make a 'super detector' covering the full solid angle. The list mode data is conventionally sorted into a 2 or higher dimension histogram, which simplifies the extraction of correlation information between the recorded coincidence events. Prior to sorting of the data into the γ^N histograms, data from different detectors are required to attain a desired energy calibration. This ensures that the data are detector independent. During the period of the experiment, possibilities of instrumental drifts cannot be excluded. These drifts has to be corrected before any further processing of the data is undertaken, since it will otherwise deteriorate the data quality. A novel method for automatic correlation for instrumental drifts in the required γ-ray spectra has been used [1, 2].

4.3. Energy Calibration and Gain Matching

The first step in processing the data was to obtain a reliable set of calibration coefficients for all the detector channels. Energy and efficiency calibrations were performed immediately before and after each experimental session. The energy calibration of the detector can be obtained from the data with radioactive source having a number of strong transitions of known energy in the region of interest. Standard ^{133}Ba and ^{152}Eu sources are placed at the target position in order to reproduce in-beam detector-target distances, and the data were taken in singles mode. For example, with a ^{152}Eu source, a two point linear calibration using the transitions at 121.78- and 1408.01-keV is generally used to provide energy calibration ion the range 0 – 2 MeV to an accuracy of 1-keV. A polynomial equation of order 2 was used to describe the relation between the γ-photon energy (E_γ) and the recoded ADC channel number x. The equation can be written as: $E_\gamma(x) = a + b.x + c.x^2$. An accurate calibration was performed using the procedures described in [1, 3].

Once the data is accurately calibrated, the next process, before the actual sorting, is to ensure that the data obtained from each detector has a constant energy description (calibration), *i.e.* the data are detector independent. The process is known as *gain matching* and could be defined as

$$\text{Gain matching channel: } x' = \frac{1}{energy\ per\ channel} E_{\gamma}, \qquad (4.1)$$

where, E_{γ} is the energy corresponding to the ADC channel x. An illustration of the gain matching process is depicted in Fig. 4.1. The Fig. 4.1(a) shows the data prior to the gain matching and Fig. 4.1(b) depicts the same data set after the gain matching. As seen from the Fig. 4.1(a), the 121-keV peak (from ^{152}Eu) occurs at different channels for 4 crystals belonging to the same Clover. After the gain matching, the same γ-ray from the 4 crystals is matched to one common channel, depending on the choice of the parameter *epc* (energy per channel).

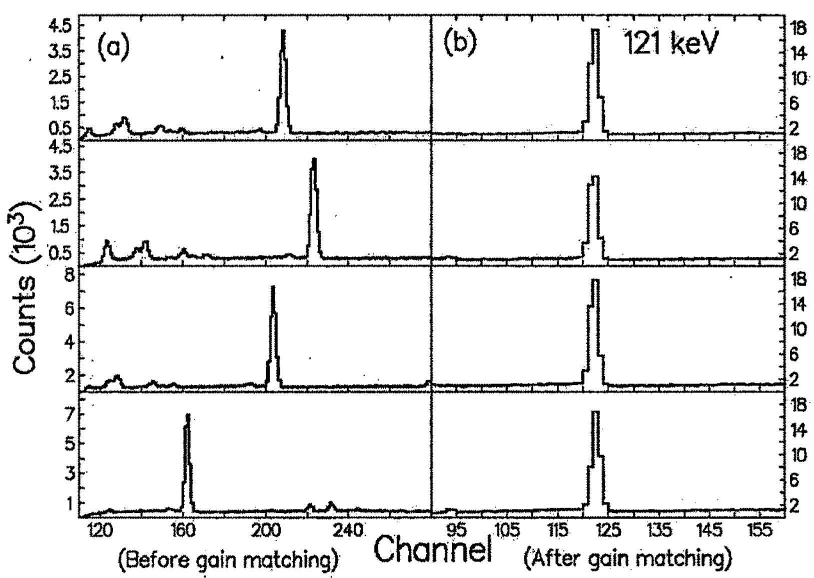

Figure 4.1: Gain matching process.

The uncalibrated spectra for all detector elements were checked for possible gain drifts. This was done by comparing the centroids of the intense 97.3-keV and 707.6-keV transitions in the ground-state band of ^{195}Tl. In order to perform these corrections there must be reference spectra (RS) in most cases obtained from the first runs for the LEPS and Clover elements (already gain matched and calibrated). The peak – shifts which are the channel differences between the reference peaks (of the RS) and the shifted peaks are determined from $(P_{1l}) - (P_{2l}) = S_l$ and $(P_{1h}) - (P_{2h}) = S_h$, where S_l and S_h are the peak – shifts in channels for one peak at the low and one peak at high energy respectively and P_{1l}, P_{1h} and P_{2h}, P_{2h} are the positions in channels of the peaks at low and high energies and P_{2h} and P_{2h} are the positions of the peaks in the reference spectrum.

The final parameters a' and b' for the Clovers were calculated using the equations below

$$a' = \frac{a(P_{2h}-P_{2l})}{(P_{2h}+S_h)-(P_{2l}+S_l)}, \tag{4.2}$$

$$b' = \frac{(P_{2l}S_h-P_{2h}S_l)}{(P_{2h}+S_h-P_{2l}-S_l)} + b\frac{(P_{2h}-P_{2l})}{(P_{2h}+S_h-P_{2l}-S_l)}, \tag{4.3}$$

where, the final parameter a' is the slope or gain and b is the old offset and b' the new offset.

The data were then sorted using the new calculated parameter a' and b' and hence the peaks were observed in the same channel number in all runs. This maintained a good energy resolution.

4.4. Doppler Shift Correction

Doppler shift corrections for the detected γ-rays were necessitated since thin targets were used for the experiments. The residual nuclei recoil into vacuum so that the detected γ-rays were subjected to energy shift according to the equation:

$$E_\gamma = E_0(1 + \beta\cos\theta), \tag{4.4}$$

where,

(i) E_γ is the Doppler shifted γ-ray energy.

(ii) E_0 is the unshifted γ-ray energy detected normal to the recoil nucleus velocity axis.

(iii) θ is the angle at which the γ-ray is detected with respect to the beam direction.

(iv) $\beta = \frac{v}{c}$, where v is the recoil velocity of the nucleus and c is the speed of light.

4.5. Analysis of Singles Data

Analysis of the singles data can be done from the one-dimensional histograms generated during sorting. Additional constraints from transitions in coincidence can be put to remove unwanted background.

The peaks associated with the discrete γ-rays ride on top of a continnum background. The background has two origins: unresolved weak transitions during the de-excitation process and imperfect response from the detector (Compton background). It is necessary to correct the background for qualitative information about the area under discrete peaks. For small regions, it is possible to estimate the background by a 'least square fit' to the data by a Gaussian peak plus polynomial background. A crude estimate of the background can be obtained by looking at the region between two peaks. For large regions, the process can be repeated to generate the background piece-wise over the whole region. There were various methods to perform the background subtraction; the one that is used here is explained by Pattabiraman *et al.*, [1, 2].

4.6. Analysis of Coincidence Data

For in-beam γ-ray spectroscopy, weak transitions are difficult to resolve in singles spectrum due to large background. Gating by another transition in coincidence with the first one can significantly reduce the background. If the singles background is taken as ~ ΔE where, ΔE is the detector resolution, the coincidence background is ~ $(\Delta E)^2$.

The main aim of the detailed data analysis is to establish the coincidence correlation between the observed γ-rays. The normal approach is to store the coincidence information in a histogram. For example, the γ-γ coincidence are stored in a 2-dimensional histograms, usually referred to as a *matrix*. Each axis of the matrix correspond to the energy of the detected γ-rays. In order to preserve the good energy resolution of Ge detectors (< 3-keV at ~1 MeV), we require atleast a 4096 x 4096 dimensional array to store the energy information. The number of counts in each (x, y) channel of the matrix tells us how many pairs of γ-rays with energy $(E_{x\gamma}, E_{y\gamma})$ have been detected.

If one is interested only in the coincidence relationship between γ-transitions, this energy correlation matrix is symmetrised by interchanging the x and y coordinated *i.e.*

$$E_{symm}(x,y) = E(x,y) + E(y,x), \tag{4.5}$$

For the analysis of angular correlation, it is necessary to generate angle dependent energy calibration and such matrices cannot be symmetrised. In γ-ray coincidence measurements, it is required that the γ-rays are detected in coincidence, that is they arrive in a short time interval, called coincidence time window. The γ-rays detected in coincidence constitute a *coincidence event*. Studying the coincidence events allows us to locate the position of the excited levels in a level scheme.

Locating the position of the γ-rays belonging to a decay path is performed by analyzing gated spectra. A gamma spectrum shows the number of detected γ-rays N with particular energy. To schematically illustrate the above process let us assume the decay scheme, as shown in Fig. 4.2. for a particular nucleus with five transitions having energies $E_{\gamma 1}$, $E_{\gamma 2}$, $E_{\gamma 3}$, $E_{\gamma 4}$, $E_{\gamma 5}$ as shown in Fig. 4.3. (Note: for simplicity same number of γ-rays are detected for all five transitions and that there is no background). A spectrum gated on $E_{\gamma 1}$ shows only the gamma rays that are detected in coincidence with γ_1. Thus, the spectrum gated in $E_{\gamma 1}$ will show peaks at $E_{\gamma 5}$, $E_{\gamma 2}$, and $E_{\gamma 4}$ which indicates that these transitions are in coincidence. The spectrum gated on $E_{\gamma 3}$ can be seen from a gate on $E_{\gamma 4}$ but not in the $E_{\gamma 1}$ and $E_{\gamma 5}$ gates which infers that the transition $E_{\gamma 3}$ is in *anti-coincidence* with the $E_{\gamma 1}$ and $E_{\gamma 5}$ transitions. Carefully placing them we could observe that the transition $E_{\gamma 3}$ has energy equal to the sum of the $E_{\gamma 1}$ and $E_{\gamma 5}$. (i.e. $E_{\gamma 3} = E_{\gamma 1} + E_{\gamma 5}$). A gate on $E_{\gamma 2}$ shows only one peak $E_{\gamma 1}$ with which it is in coincidence but in anticoincidence with all other transitions. We go through all the gated spectra again and check that they are consistent with our new level scheme.

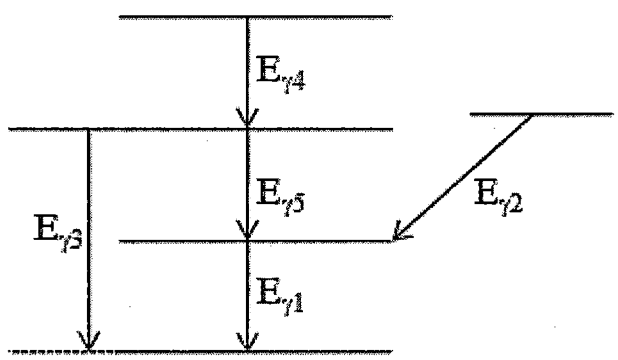

Figure 4.2: A simple level scheme of 5 γ-ray transitions.

4.7. Assignment of Spin and Parity

The excited states of a nucleus are characterised by their excitation energy E^*, spin J and parity π. For the electromagnetic decay from the initial state (E_i, J_i, π_i) to the final state (E_f, J_f, π_f) the resultant electromagnetic radiation must satisfy the following conditions:

Energy E_γ of the photon	$E_\gamma = E_i - E_f$
Angular momentum L carried by the photon	$J_i + J_f \geq L \geq \lvert J_i - J_f \rvert$
Component of L along the quantization direction	$M = M_i - M_f$
Photon Parity π	$\pi = \pi_i \pi_f$

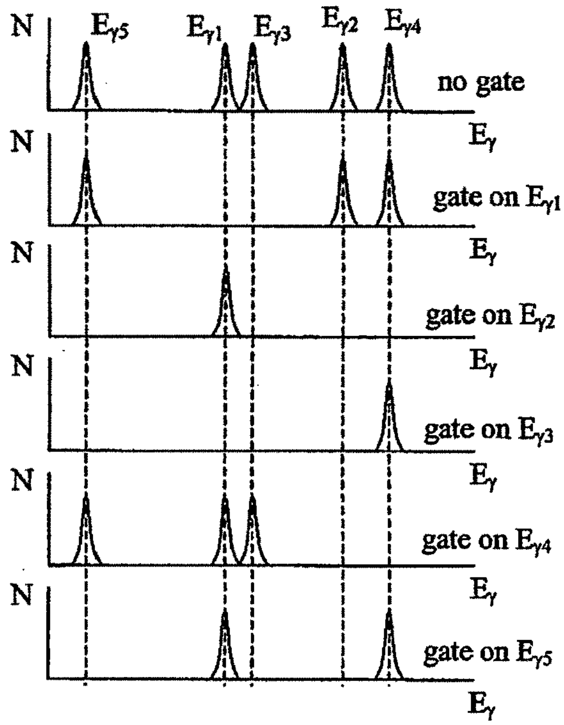

Figure 4.3: Schematic γ-ray spectra with different gating conditions corresponding to the level scheme of figure above.

For in-beam spectroscopy, levels are usually fed from entry channels that are high in excitation energy and spin. The subsequent de-excitation process leads to the population of a series of bands with strong inter-band transitions. Assignment of spin-parity within a band is generally done on the basis of the following assumptions. (i) level spin monotonically decreases with decreasing excitation energy (ii) due to side-feeding, the population of a level increases with decreasing excitation energy (iii) all the levels within a band are of the same parity (with the exception of nuclei with octupole deformation having enhances E1 rates). Independent confirmation of the spin parity assignment is possible if additional inter-band transitions feeding or decaying from the level of interest can also be identified.

4.7.1. Directional Correlations from Oriented States (DCO)

The fixed angular granularity of modern γ-ray arrays and the complexity of the singles spectra may not provide a feasible situation for a complete angular distribution analysis from the singles spectra. The coincidence angular γ-γ measurements have a distinct advantage over the single measurements due to a substantial reduction in the background as well as a reduction in the contamination from other sources.

In this method, measurements can be carried out with a minimum of two detectors with one at ~ 0°/180° and the other at ~ 90° [4]. If the detectors are sensitive to both radiations γ_1 and γ_2, we can distinguish between (i) γ_1 in detector 1 and γ_2 in detector 2 and (ii) γ_2 in detector 1 and γ_1 in detector 2. DCO ratio is defined as the ratio between the coincidence count rates

$$DCO = {W(\gamma_1, \theta_1; \gamma_2, \theta_2)}\Big/{W(\gamma_1, \theta_2; \gamma_2, \theta_1)}, \qquad (4.6)$$

The coincidence intensity is determined as $I_{\gamma\gamma}(\theta_1, \theta_2)$ and $I_{\gamma\gamma}(\theta_2, \theta_1)$ by detecting γ-rays at θ_1 when gated by the other γ-ray of known multipolarity at θ_2 and vice-versa, respectively. In the present work multipolarity of the de-exciting γ-rays were deduced from the observed γ-ray coincidence angular correlation [5, 6]. For the INGA data, the coincidence data were sorted into asymmetric angle dependent matrix whose one axis correspond to the γ-ray energy deposited in the detectors at 90° while the other axis correspond to the γ-ray energy deposited in the detectors at 40°. A gate corresponding to a γ-ray of known multipolarity was made on one axis (say x-axis) and the coincidence spectrum was projected on the other (y-axis). The same gate was then set on the y-axis and the projection was made on x-axis. Assuming stretched transitions, the intensities of the transitions which had the same multipolarity as the gated γ-rays were approximately the same in both the spectra. However, the intensities differed by a factor of ~ 2 for transitions of a different multipolarity. The observed values of R_{DCO} in the INGA data are illustrated in Fig. 4.4. The R_{DCO} value is ~ 0.88 for dipole and ~ 1.6 for quadruple transitions when gated on a pure dipole transition.

The main advantage of the DCO ratio is that since both γ - γ combinations are collected simultaneously; systematic errors from beam normalization and detector efficiency are cancelled out. Having determined the spins of all the transitions in the level scheme, the spin assignment of the underlying states is done on the basis of the assumption that γ-ray de-excitation takes place from a state with initial spin J_i to a state J_f (i.e. $J_f \rightarrow J_i$). The details of the DCO analysis in the present work are explained in detail in Chapter 5 and 6.

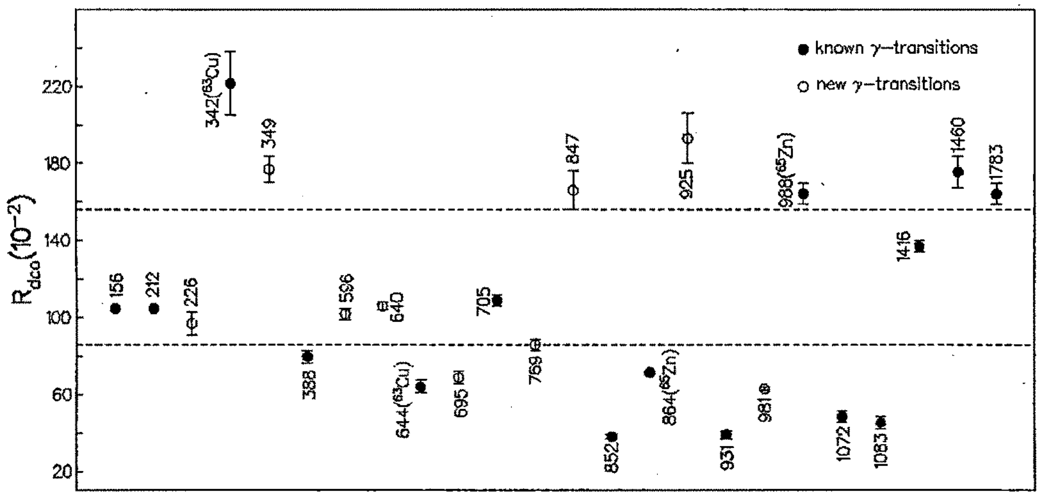

Figure 4.4: Gamma-ray asymmetry R_{DCO} plotted as a function of the γ-ray energy. The lines have been drawn to guide the eye correspond to the average values of ~ 0.88 for a dipole transition and ~ 1.6 for quadruple transition when gated on a pure dipole transition. The quoted errors include the errors due to background subtraction, fitting and efficiency correction.

4.7.2. Linear Polarization Measurements

The determination of spins and parities based on the radiation patterns of the emitting nucleus using directional correlation from oriented states (DCO) often assumes that the emitted radiations are *pure* and *stretched* in character. However, if some form of mixing is present, the R_{DCO} value is perturbed. A further ambiguity arises from the fact that the R_{DCO} value does not provide information on the electromagnetic nature of the transition, as the angular distribution for an electric and a magnetic multipole radiation of the same order are identical. These ambiguities can be uniquely resolved by measuring the linear polarization of the γ-ray transitions.

Linear polarization measurement, *i.e.* the direction of the electric vector with respect to the beam detector plane distinguishes the electric and magnetic nature of the γ-ray. The linear polarization measurements were performed using the INGA and

AFRODITE Clover detector. Multi-Clover array facilitated coincidence polarization measurements [7, 8, 9]. This method has a unique advantage of reducing the contamination from neighbouring nuclei and background, thereby helps in relatively unambiguous assignment for the parity of the states whose spin value is already known.

4.7.3. Clover Detector as a Polarimeter

For photons of ~ 1 MeV energy range, Compton scattering process is the most dominant mechanism for the interaction with the electrons in the scattering medium. The plane of polarization of the incident radiation can be obtained by comparing the ratio of photons scattered in-plane ($N_{\parallel}$) and in a perpendicular plane ($N_{\perp}$). Since the polarization sensitivity is maximum at $\theta = 90°$ we need an efficient detection system for the identification of photons scattered in mutually perpendicular direction.

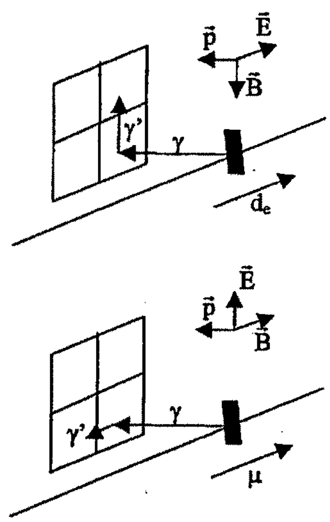

Figure 4.5: Compton scattering in a Clover detector for stretched electric (top panel) and magnetic (bottom panel) dipole transition.

There are various configurations of Compton - polarimeters in literature [10 - 15] that use Ge crystals both as scatterer and absorber. In the Clover design [16], four HPGe crystals are arranged in a Clover leaf pattern within the same cryostat. In Compton scattering the largest number of γ-rays are scattered perpendicular to the direction of the $\vec{E}$ vector, thus the scattered γ-ray γ' has the largest probability to propagate in vertical direction towards the top of right crystal of the Clover detector (ref Fig. 4.5). In this case one part of the initial energy of the γ-ray ($E_\gamma - E_{\gamma'}$) is deposited in the bottom right crystal, while the second part ($E_{\gamma'}$) is collected in the right top right crystal. These events are known as *double-hit events*. Thus for electric dipole transition the majority of the double-hit events will be registered in the vertically placed crystals of the Clover detectors. For magnetic dipole transition (Fig. 4.5) the scattered γ-ray γ' has the largest probability to propagate perpendicular to $\vec{E}$, that is in the horizontal direction, *i.e.* towards the bottom left crystal of the Clover detector. Thus, for magnetic dipole transitions the majority of the double-hit events will be registered in the horizontally placed crystals of the Clover detectors.

4.7.4. Polarization Matrix

A polarization matrix, using the procedure described in Refs. [8, 9] was constructed from the data where the energy recorded in any detector was placed on one axis, while the other axis corresponded to the energy scattered in a perpendicular or parallel segment of the Clover with respect to the beam axis. From the projected spectra, the number of perpendicular ($N_\perp$) and parallel ($N_{||}$) scatters for a given γ-ray can be obtained. From these spectra the asymmetry parameter Δ_{IPDCO} was obtained using the relation:

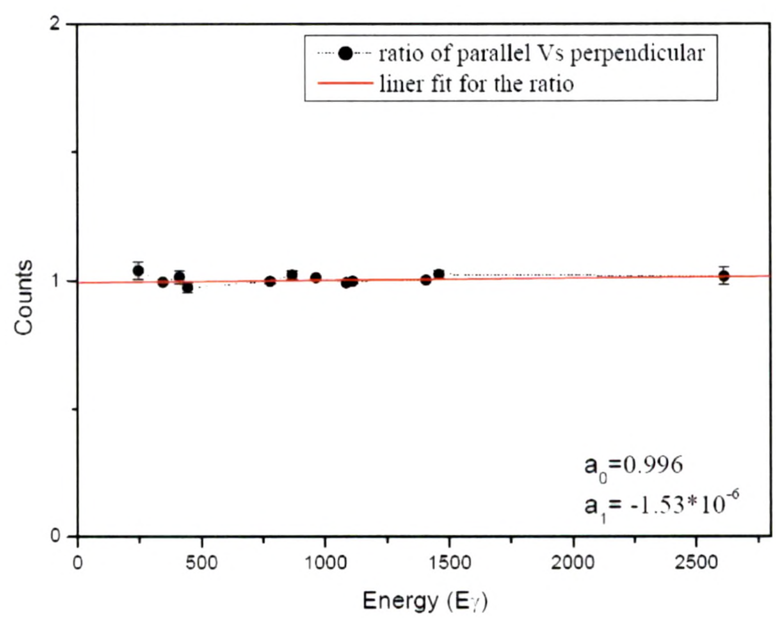

Figure 4.6: The figure shows the correction parameter *a*, as a function of the γ-ray energy for the INGA experiment.

$$\Delta_{IPDCO} = \frac{(a(E_\gamma)N_\perp) - N_\parallel}{(a(E_\gamma)N_\perp) + N_\parallel}, \tag{4.7}$$

The correction parameter 'a' is due to the asymmetry of the experimental configuration. This correction parameter is deduced from the radioactive sources, where the number of parallel and perpendicular events would be same; due to isotropic nature of the emitted radiations. The correction parameter could be expressed as a function of the γ-ray energy, *i.e.*

$$a(E_\gamma) = a_0 + a_1 E_\gamma, \tag{4.8}$$

where, a_0 = 0.996 and a_1 = -1.53 x 10^{-6} $(\text{keV})^{-1}$. The value of a_0 remains almost constant in the energy range 121- to 1408-keV, as shown in Fig. 4.6.

A pure electric transition due to its preferential scattering in the perpendicular direction with respect to the beam axis results in a positive value for Δ_{IPDCO}. Similarly a pure magnetic transition results in a negative value for Δ_{IPDCO} due to its preferential scattering along the parallel direction and a near-zero value for Δ_{IPDCO} is indicative of an admixture.

References:

1. N.S. Pattabiraman, S.N. Chintalapudi, S.S. Ghugre, Nucl. Instrum. Methods Phys. Res. A 526, 439 (2004)
2. N.S. Pattabiraman, S.N. Chintalapudi, S.S. Ghugre, Nucl. Instrum. Methods Phys. Res. A 526, 432 (2004)
3. N.S. Pattabiraman, Ph.D Thesis, Calcutta University, India, 2004 (Unpublished)
4. A. Krämer-Flecken, T. Morek, R.M. Leider, W. Gast, G. Hebbinghaus, H.M. Jäger, W. Urban, Nucl. Instrum. Methods Phys. Res. A 275, 333 (1989)
5. F.S. Stephens, M.A. Delenplanque, R.M. Diamond, A.O. Macchiavelli, J.E. Draper, Phys. Rev. Lett. 54, 2584 (1985)
6. C.W. Beausang, D. Prévost, M.H. Bergström, G. de France, B. Haas, J.C. Lisle, Ch. Theisen, J. Timár, P.J. Twin, J.N. Wilson, Nucl. Instrum. Methods Phys. Res. A 364, 560 (1995)
7. G. Duchêne, F.A. Beck, P.J. Twin, G. de France, D. Curien, L. Han, C.W. Beausang, M.A. Bentley, P.J. Nolan, J. Simpson, Nucl. Instrum. Methods Phys. Res. A 432, 90 (1999)
8. Ch. Droste, K. Starosta, A. Wierzchucka, T. Morek, S.G. Rohozinskii, J. Srebrny, M. Bergstrom, B. Herskind, E. Wesolowski, Nucl. Instrum. Methods Phys. Res. A 337, 430 (1999)
9. K. Starosta *et al.,* Phys. Rec. C 69, 044317 (2002)
10. R. Bass *et al.,* Nucl. Instrum. Methods Phys. Res. 163, 377 (1979)
11. J. Simpson, P.A. Butler, Nucl. Instrum. Methods Phys. Res. 204, 463 (1983)
12. P.M. Jones *et al.,* Nucl. Instrum. Methods Phys. Res. A 362, 556 (1995)
13. L.M. Garcia-Raffi *et al.,* Nucl. Instrum. Methods Phys. Res. A 391, 461 (1997)
14. G. J. Schmid *et al.,* Nucl. Instrum. Methods Phys. Res. A 417, 95 (1998)
15. C. Hutter *et al.,* Nucl. Instrum. Methods Phys. Res. A 489, 247 (2002)
16. G. Duchene *et al.,* Proc. Workshop on Large Gamma-Ray Detector Arrays, Chalk River, Canadan May 1992, AECL 10613 (1992)